

Deeply virtual electroproduction of photons and mesons on the nucleon

M. Vanderhaeghen^a, P.A.M. Guichon^b and M. Guidal^c

^aInstitut für Kernphysik, University of Mainz, D-55099 Mainz, Germany

^bService de Physique Nucléaire, CEA/Saclay, F-91191 Gif-sur-Yvette, France

^cInstitut de Physique Nucléaire - IN2P3, F-91406 Orsay, France

We give predictions for the leading order amplitudes for deeply virtual Compton scattering and hard meson electroproduction reactions at large Q^2 in the valence region in terms of skewed quark distributions. We give first estimates for the power corrections to these leading order amplitudes. In particular, we outline examples of experimental opportunities to access the skewed parton distributions at the current high-energy lepton facilities : JLab, HERMES and COMPASS.

In recent years, a unified theoretical description of a wide variety of exclusive processes in the Bjorken regime has emerged through the formalism introducing new generalized parton distributions, the so-called skewed parton distributions (SPD's). It has been shown that these distributions, which parametrize the structure of the nucleon, allow to describe in leading order perturbative QCD (PQCD), various exclusive processes such as, in particular, deeply virtual Compton scattering (DVCS) and longitudinal electroproduction of vector and pseudoscalar mesons (see e.g. Refs.[1]-[4] and references therein).

The leading order PQCD diagrams for DVCS and hard meson electroproduction are of the type as shown in Fig. 1. It has been proven [1,2] that the leading order DVCS ampli-

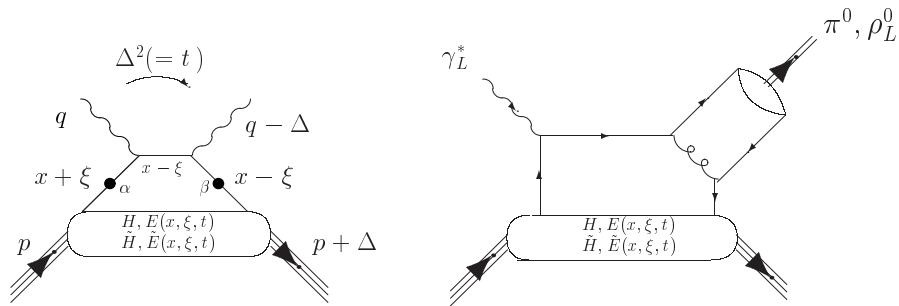


Figure 1. Leading order diagrams for DVCS (left) and for longitudinal electroproduction of mesons (right).

tude in the forward direction can be factorized in a hard scattering part (which is exactly calculable in PQCD) and a soft, nonperturbative nucleon structure part as is illustrated

on the left panel of Fig. 1. The nucleon structure information can be parametrized, at leading order, in terms of 4 generalized structure functions. In the notation of Ji, these functions are the off-forward parton distributions (OFPD's) denoted as $H, \tilde{H}, E, \tilde{E}$ which depend upon three variables : x, ξ and t . The light-cone momentum fraction x is defined by $k^+ = xP^+$, where k is the quark loop momentum and P is the average nucleon momentum (using the definition $a^\pm \equiv 1/\sqrt{2}(a^0 \pm a^3)$). The skewedness variable ξ is defined by $\Delta^+ = -2\xi P^+$, where Δ is the overall momentum transfer in the process and where $2\xi \rightarrow x_B/(1 - x_B/2)$ in the Bjorken limit. Furthermore, the third variable entering the OFPD's is given by the Mandelstam invariant $t = \Delta^2$. In Fig. 1, the variable x runs from -1 to 1. As noted by Radyushkin [2], one can identify two regions for the SPD's. In the regions where $x > \xi$ or $x < -\xi$, the SPD's are the generalizations of the usual parton distributions from DIS. Actually, in the forward direction, the OFPD's H and \tilde{H} respectively reduce to the quark density distribution $q(x)$ and quark helicity distribution $\Delta q(x)$, obtained from DIS. In the region $-\xi < x < \xi$, the SPD's behave as a “meson-like” distribution amplitude and contain new information about nucleon structure [5].

To provide estimates for electroproduction observables, we need a model for the SPD's. The following calculations were performed using ξ -dependent SPD's based on a product ansatz (for the double distributions [6]) of a quark distribution (we use the MRST98 quark distributions [7] as input) and an asymptotic “meson-like” distribution amplitude (see Ref. [9] for more details). The t -dependence is given by the corresponding form factors (Dirac form factor for H , axial form factor for \tilde{H}).

Besides the DVCS process, a factorization proof was also given for the leading order meson electroproduction amplitude in the valence region at large Q^2 [3], which is shown on the right panel of Fig. 1. This factorization theorem only applies when the virtual photon is longitudinally polarized. The leading order longitudinal amplitude for meson electroproduction behaves as $1/Q$. This leads to a $1/Q^6$ scaling behavior for the longitudinal cross section $d\sigma_L/dt$ at large Q^2 , which provides an experimental signature of the leading order mechanism. Besides the dependence on the SPD's, the meson electroproduction amplitudes require the additional non-perturbative input from the meson distribution amplitudes, for which we take asymptotic forms in the calculations. Furthermore, it was shown in Ref.[3] that electroproduction of vector (pseudoscalar) mesons accesses the unpolarized (polarized) OFPD's H and E (\tilde{H} and \tilde{E}) respectively. According to the produced meson ($\rho^0, \rho^\pm, \omega, \phi, \pi^0, \pi^\pm, \eta, \dots$), the SPD's for the different quark flavors enter in different combinations due to the different quark charges and isospin factors.

We show here some results for DVCS and meson electroproduction observables using the ξ -dependent ansatz for the OFPD's described previously. For more results, we refer to our works in Refs.[4,8,9]. In Fig. 2, the ρ_L^0, π^+ and γ cross sections are compared as function of the beam energy at fixed Q^2 in the valence region. Going up in energy, the increasing virtual photon flux factor boosts the meson leptonproduction cross sections and the DVCS part of the γ leptonproduction cross section. Comparing the different channels, it is clear on this picture that the ρ_L^0 channel is very favorable as it depends on the unpolarized SPD's. For the γ channel, the contaminating Bethe-Heitler (BH) process is hardly influenced by the beam energy and therefore overwhelms the DVCS cross section at low beam energies. Although Fig. 2 shows that a high energy such as planned at COMPASS is preferable, one can try to undertake a preliminary study of the hard electroproduction reactions using

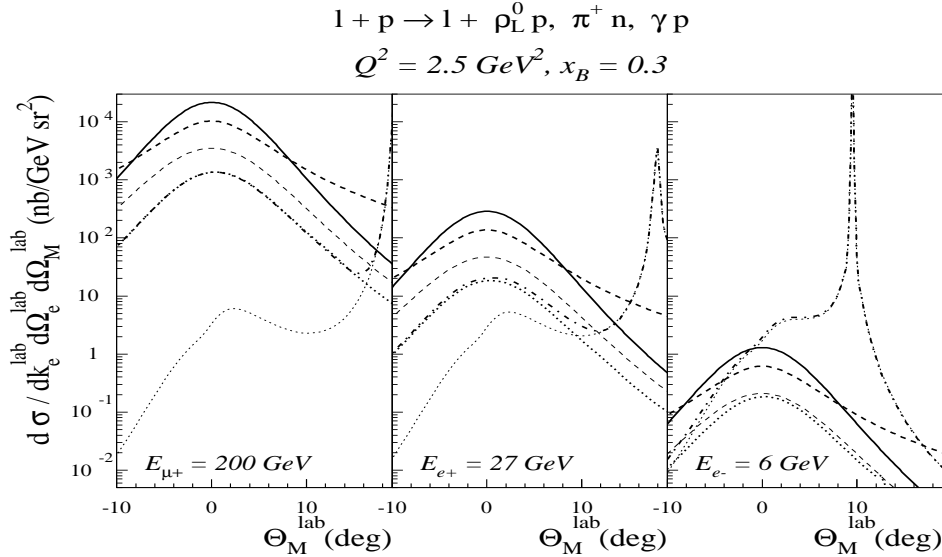


Figure 2. Comparison between the angular dependence of the leading order predictions for the ρ_L^0 (full lines), π^+ (thick, upper dashed lines) leptonproduction and DVCS (thick dotted lines) in-plane cross sections at $Q^2 = 2.5 \text{ GeV}^2$, $x_B = 0.3$ and for different beam energies : $E_{\mu^+} = 200 \text{ GeV}$ (COMPASS), $E_{e^+} = 27 \text{ GeV}$ (HERMES), $E_{e^-} = 6 \text{ GeV}$ (JLab). The BH (thin dotted lines) and total γ (dashed-dotted lines) cross sections are also shown. For the π^+ , the result excluding the pion pole is also shown (thin, lower dashed lines).

the existing facilities such as HERMES or JLAB, despite their low energy. Recently, an experiment has been approved at JLAB [10] to investigate (the onset of) the scaling behavior for ρ_L^0 electroproduction in the valence region ($Q^2 \approx 3.5 \text{ GeV}^2$, $x_B \approx 0.3$).

Although at present, no experimental data for the ρ_L^0 electroproduction at larger Q^2 exist in the valence region ($x_B \approx 0.3$), the reaction $\gamma^* p \rightarrow \rho_L^0 p$ has been measured at smaller values of x_B . We therefore compare our results in Fig. 3 to see how these data approach the valence region, where one is sensitive to the quark SPD's. For the purpose of this discussion, we call the mechanism which proceeds through the quark SPD's, the Quark Exchange Mechanism (QEM). Besides the QEM, ρ^0 electroproduction at large Q^2 and small x_B proceeds predominantly through a perturbative two-gluon exchange mechanism (PTGEM) as studied in Ref. [11]. To compare to the data at intermediate Q^2 , we implemented in both mechanisms the power corrections due to the parton's intrinsic transverse momentum dependence (see Ref. [9] for details), which give a significant reduction at the lower Q^2 values. Comparing our results with the data in Fig. 3, one sees that the PTGEM explains well the fast increase at high c.m. energy (W) of the cross section but substantially underestimates the data at lower energies. This is where the QEM is expected to contribute since x_B is then in the valence region. The QEM describes well the change of behavior of the data at lower W . This has also been confirmed by recent HERMES data (around $W \approx 5 \text{ GeV}$) [12] to which we compared our calculations.

It is clear that at present new and accurate data for these exclusive channels are needed. The fundamental interest of the SPD's justifies an effort towards their experimental determination in order to open up a new domain in the study of the nucleon structure.

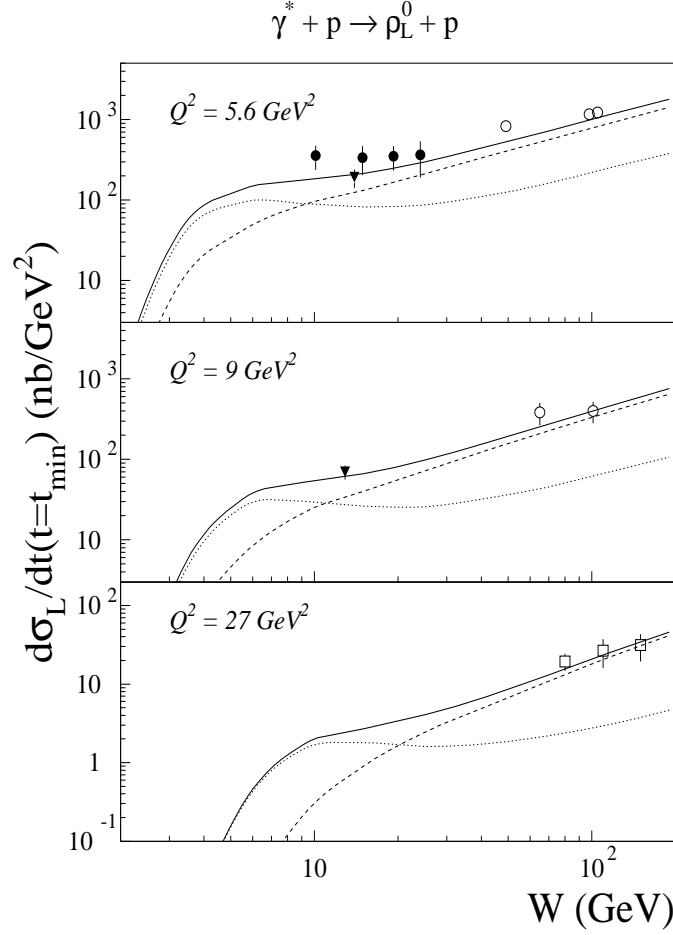


Figure 3. Longitudinal forward differential cross section for ρ_L^0 electroproduction. Calculations compare the quark exchange mechanism (dotted lines) with the two-gluon exchange mechanism (dashed lines) and the sum of both (full lines). Both calculations include the corrections due to intrinsic transverse momentum dependence. The data are from NMC (triangles), E665 (solid circles) and ZEUS (open circles and squares). References to the data can be found in Ref. [9].

REFERENCES

1. X. Ji, Phys.Rev.Lett. **78**, 610 (1997); Phys.Rev.D **55**, 7114 (1997).
2. A.V. Radyushkin, Phys.Lett.B **380**, 417 (1996); Phys.Rev.D **56**, 5524 (1997).
3. J.C. Collins, L. Frankfurt and M. Strikman, Phys.Rev.D **56**, 2982 (1997).
4. P.A.M. Guichon and M. Vanderhaeghen, Prog.Part.Nucl.Phys. **41**, 125 (1998).
5. M.V. Polyakov and C. Weiss, hep-ph/9902451.
6. A.V. Radyushkin, Phys.Rev.D **59**, 014030 (1999).
7. A.D. Martin, R.G. Roberts, W.J. Stirling, R.S. Thorne, Eur. Phys. J. C **4**, 463 (1998).
8. M. Vanderhaeghen, P.A.M. Guichon and M. Guidal, Phys.Rev.Lett. **80**, 5064 (1998).
9. M. Vanderhaeghen, P.A.M. Guichon and M. Guidal, Phys.Rev.D (1999), in press; hep-ph/9905372.
10. JLab exp. E98-107/E99-105, spokespersons M. Guidal, C. Marchand and E. Smith.
11. L. Frankfurt, W. Koepf and M. Strikman, Phys.Rev.D **54**, 3194 (1996).
12. G. van der Steenhoven, these proceedings.